Supporting Information

Gadêlha et al. 10.1073/pnas.1302113110

SI Text

1. Parameter Estimation from Flagellar Axoneme Experiments

We focus our dimensional analysis on the typical physical quantities found in experimental models of flagellar axonemes, which are commonly extracted from sea urchin sperm and *Chlamydomonas* due to the absence of accessory structures in their flagella. In demembranated sperm flagella of the sea urchin *Lytechinus pictus*, in the presence of ATP and vanadate, the flexural rigidity has been reported to be $E_b = 0.9 \times 10^{-21}$ Nm^2 (1–3), whereas the interdoublet elastic resistance from demembranated flagellar axonemes of *Chlamydomonas*, equally in the presence of ATP, yields an estimated spring constant of 2.0×10^{-3} N/m for 1 μm of axoneme (4). If the diameter of the axoneme is assumed to be $b = 185$ nm, with a total length of $L = 35$ μm, as typically found in the sea urchin flagellum (5), the dimensionless sliding resistance parameter,

$$\mu = L^2 \left(\frac{b^2 K}{E_b} \right), \qquad \text{[S1]}$$

is ∼93, reaching values as high as $\mu \approx 150$ for an increment of only 10 μm in the total flagellar length, due to its sensitivity to the length scale L. In addition, a good correspondence with the above estimate of the sliding resistance, μ, is found when we consider direct measurements of the relative ratio between the bending rigidity and the interfilament sliding resistance instead. This is estimated to be $b^2 K / E_b \sim 0.03 - 0.08/\mu\text{m}^2$ for a demembranated sea urchin flagellar axoneme (5), which results in a slip resistance number varying from $\mu \approx 36$ to $\mu \approx 98$. Surprisingly, similar estimates for μ can also be derived from data on the bull sperm flagellum (6), despite its additional structural elements, such as the outer dense fibers and fibrous sheath. Indirect calculations via model curve fitting of extracted flagellar bending waves from live bull sperm swimming in watery medium yield estimates of $E_b = 1.7 \times 10^{-21}$ Nm^2, a sliding resistance of -1580 N/m^2, and a basal compliance of -93.6×10^{-3} N/m (6). The details of the negative signs for the estimated sliding resistance and basal compliance are explained by specific model assumptions in the study by Riedel-Kruse et al. (6). However, if we consider the absolute value of their estimates, together with the dimensional parameters used by Riedel-Kruse et al. (6) for the model curve fitting, that is, $L = 58.3$ μm and $b = 185$ nm, the resulting dimensionless sliding resistance and basal compliance numbers are given by, respectively, $\mu \approx 108$ and $\gamma \approx 0.5$.

Intrinsic uncertainties from modeling simplifications are, however, present for each of the experimental measurements discussed above. Flexural experiments to extract the axonemal bending rigidity categorically neglected the mechanical influence of the passive cross-linking proteins (1–3), whereas the possible mechanical effect of a compliant base was not taken into account for measurements of the axonemal interdoublet elasticity (4) or during direct evaluation of the relative ratio between K and E_b (5). In particular, Pelle et al. (5) considered a simplified scenario for the bending moments acting within the passive region during curve-fitting routines by neglecting both the nonlocal effects of the basal compliance on the passive section and the intrinsic coupling between the passive and active regions (equation 6 in ref. 5). As a consequence, the final expression (equation 10 in ref. 5) is not a formal solution of the original boundary value problem (equation 6 in ref. 5) and depends on two unknown constants that are disconnected from the biophysical quantities of system, whereas the repercussions of using an incomplete solution during curve fitting with empirical counterbend data are not known. In fact, these ad hoc constants within the study by Pelle et al. (5) are well-defined quantities of the problem, as demonstrated in our formalism. Likewise, it is not clear whether fitting dimensional parameters using large-amplitude bending waves and geometrically linear mathematical models, which assume small deflections (6), are legitimate or accurate. Furthermore, Riedel-Kruse et al. (6) did not consider the tapering of the additional structural elements found in bull sperm flagella, such as outer dense fibers and the fibrous sheath, which gradually reduce down the flagellum diameter and are absent close to the end piece (7–9); instead, a constant bending rigidity along the flagellum length was assumed during the parameter-fitting routine. In contrast, the bull sperm flagellum stiffness is proximally observed to be much greater than the sea urchin flagellar axoneme, with a monotonic decrease to a small fraction of its maximum in the distal region (10).

Here, we consider the sliding resistance parameter varying from $\mu = 0$ to $\mu = 100$ and a basal compliance number bounded in $0 \leq \gamma \leq 1$, as detailed in the main text. This parameter range is sufficient to scrutinize the mechanical effects instigated by the sliding cross-linking resistance and the basal compliance in a general setting while studying a physiologically relevant parameter regime. Nevertheless, intrinsic uncertainties are present in each experimental measurement discussed above (1, 2, 4–6) due not only to inherent experimental noise but, and most importantly, to model simplifications while extracting empirical quantities.

1. Okuno M, Hiramoto Y (1979) Direct measurements of the stiffness of echinoderm sperm flagella. *J Exp Biol* 79(1):235–243.
2. Okuno M (1980) Inhibition and relaxation of sea urchin sperm flagella by vanadate. *J Cell Biol* 85(3):712–725.
3. Howard J (2001) *Mechanics of Motor Proteins and the Cytoskeleton* (Sinauer, Sunderland, MA).
4. Minoura I, Yagi T, Kamiya R (1999) Direct measurement of inter-doublet elasticity in flagellar axonemes. *Cell Struct Funct* 24(1):27–33.
5. Pelle DW, Brokaw CJ, Lesich KA, Lindemann CB (2009) Mechanical properties of the passive sea urchin sperm flagellum. *Cell Motil Cytoskeleton* 66(9):721–735.
6. Riedel-Kruse IH, Hilfinger A, Howard J, Jülicher F (2007) How molecular motors shape the flagellar beat. *HFSP J* 1(3):192–208.
7. Fawcett DW, Bloom W, Raviola E (1994) *A Textbook of Histology* (Chapman & Hall, New York).
8. Fawcett DW (1975) The mammalian spermatozoon. *Dev Biol* 44(2):394–436.
9. Gaffney EA, Gadêlha H, Smith DJ, Blake JR, Kirkman-Brown JC (2011) Mammalian sperm motility: Observation and theory. *Annu Rev Fluid Mech* 43:501–528.
10. Lesich KA, Pelle DW, Lindemann CB (2008) Insights into the mechanism of ADP action on flagellar motility derived from studies on bull sperm. *Biophys J* 95(1): 472–482.

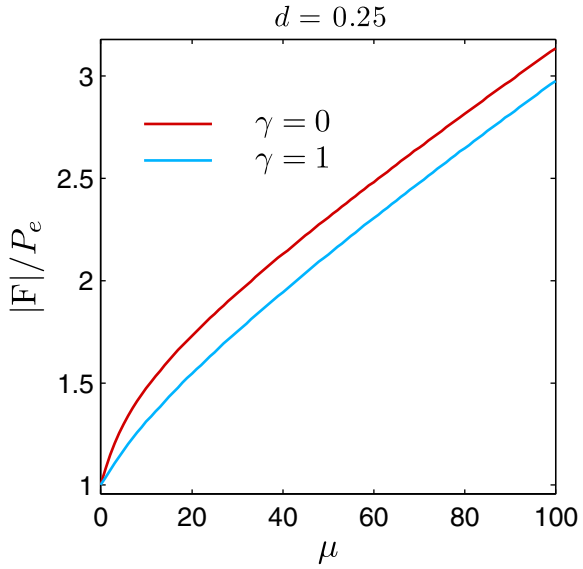

Fig. S1. Actuation force magnitude, $|\mathbf{F}|$, relative to the associated Euler bucking load P_e, as a function of the sliding resistance parameter, μ, for two values of the basal compliance parameter, γ, for a constant horizontal displacement, $d = 0.25$. Note that different material parameters (μ, γ) may have identical force magnitude $|\mathbf{F}|$ for a given displacement d.